J. Water Environ. Nanotechnol., 5(1): 34-44 Winter 2020

ORIGINAL RESEARCH PAPER

Trinitroanisole Adsorption on the Surface of Boron Nitride Nanocluster ($B_{12}N_{12}$): A Computational Study

Mohammad Reza Jalali Sarvestani[1] and Roya Ahmadi[2,*]

[1] Young Researchers and Elite Club, Yadegar-e-Imam Khomeini(RAH) Shahr-e-Rey Branch, Islamic Azad University, Tehran, Iran

[2] Department of Chemistry, Yadegar-e-Imam Khomeini (RAH) Shahre-rey Branch, Islamic Azad University, Tehran, Iran

Received: 2019-11-08 Accepted: 2019-12-27 Published: 2020-02-01

ABSTRACT

This paper investigated boron nitride nanocage performance as an adsorbent and sensing material for removal and detection of trinitroanisole by density functional theory. The calculated adsorption energies, Gibbs free energy changes (ΔG_{ad}), adsorption enthalpy changes (ΔH_{ad}), and thermodynamic equilibrium constants (K_{th}) revealed the adsorption process is experimentally feasible, spontaneous, exothermic and Irreversible. The highly negative adsorption energy values and bond lengths between $B_{12}N_{12}$ and trinitroanisole indicated the interaction between the adsorbate and the adsorbent is a chemisorption process and the NBO results also confirmed covalent bonds are formed between trinitroanisole and the adsorbent in all of the evaluated conformers. The N-O and C-N bond lengths and the density values showed that trinitroanisole complexes with boron nitride cage have higher explosive velocity and detonation pressure than the pure trinitroanisole without $B_{12}N_{12}$. The frontier molecular orbital parameters such as bandgap, chemical hardness, electrophilicity, chemical potential, and charge capacity were also studied and the findings proved $B_{12}N_{12}$ is an excellent sensing material for fabricating novel electrochemical and thermal sensors for detection of trinitroanisole. All of the performed computations in this study were done in very similar situations to the real operational conditions such as considering water as the solvent and checking the effect of temperature on the adsorption efficiency. In addition, all of the calculations were done using the DFT method and B3LYP/6-31G(d) level of theory which its results are usually inadmissible following the experimental findings.

Keywords: *Nitroaromatic explosives, DFT, Adsorption, Boron nitride cage, Detection*

How to cite this article

Jalali Sarvestani MR, Ahmadi R.Trinitroanisole Adsorption on the Surface of Boron Nitride Nanocluster ($B_{12}N_{12}$): A Computational Study. J. Water Environ. Nanotechnol., 2020; 5(1): 34-44. DOI: 10.22090/jwent.2020.01.003

INTRODUCTION

Nitroaromatic explosives are potential environmental contaminants which their removal and detection are very important [1-3]. Trinitroanisole (Fig. 1) is a nitroaromatic energetic compound that causes several problems to the people exposed to it including different types of cancer, cataracts, skin rashes, nose bleeds, anemia, hepatotoxicity, vomiting, vitiligo and weight loss [4-6]. The former researches proved that the people who live or work near the ammunition plants, drowned warships, military munition sites, and war-torn countries are potential victims for diseases associated with nitroaromatic explosives [7-9]. When a nitroaromatic compound enters the body of a living organism, nitroanion radicals synthesized in the body which causes oxidation stress by their redox recycling and induce their mutagenic and carcinogenic effects by this mechanism [10].

Several techniques have been reported for quantitation of nitroaromatic explosives including high-performance liquid chromatography (HPLC), gas chromatography (GC), fluorescence spectros-

* Corresponding Author Email: *roya.ahmadi.chem@gmail.com*

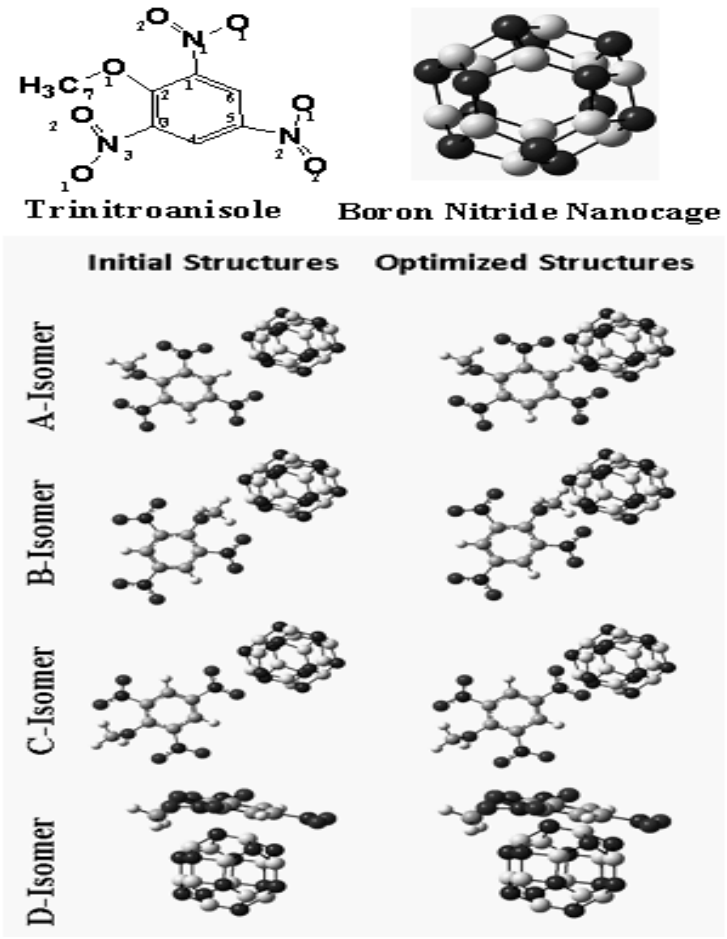

Fig. 1. The optimized structures of boron nitride cage and its complexes with trinitroanisole

copy, and mass spectrometry (MS) [11-13]. Unfortunately, these methods require a very expensive instrument and sophisticated operators. Moreover, they are time-consuming and consumes a lot of organic solvents. On the other hand, thermal and electrochemical sensors are small, portable, simple, and economical devices that have gained huge attention in the recent decade to themselves [14-17]. These sensors are applicable for colored specimens and their analysis time is too short. Sensors consist of a recognition element and a transducer. When the analyte interacts with the recognition element a physicochemical parameter like potential, temperature, conductivity and pH experience a sharp change in the microenvironment near the surface of the sensor then this phenomenon is altered to an electrical signal by the transducer which has a linear relationship with the analyte concentration [18-22]. Therefore, the first step in the construction of a new sensor is to find a sensing material that has a strong and selective interaction with the analyte. Some adsorbents have also been synthesized for the removal of nitroaromatic explosives but most of them suffer from low adsorption capacity and low recycling numbers [23-25]. Hence, finding a new adsorbent and sensing material for removal and detection of nitroaromatic energetic compounds is very important [26-29].

Moreover, boron nitride cage is a nanostructure with special features like high thermal stability, low dielectric constant, great thermal conductance, oxidation resistance, specific surface/area ratio, and prominent structural stability which make it an appropriate adsorbent for the removal of environmental contaminants and a good candidate for the quantitation of several analytes so that the adsorption of HCN, OCN^-, amphetamine, proline amino acid and tetryl on the surface of boron nitride cage has been investigated [30-32].

The next matter that supports evaluating the adsorption of trinitroanisole on the surface of $B_{12}N_{12}$ is that some of the previously reported studies indicated nanomaterials can improve the reactivity and energetic features of explosives and reduce their heat sensitivity in some cases [33-37]. Therefore, the aim of this study is to investigate the adsorption of trinitroanisole on the surface of $B_{12}N_{12}$ by density functional theory, for the first time.

COMPUTATIONAL DETAILS

GuassView 6 and Nanotube modeler 1.3.0.3 software was used for designing the structures of trinitroanisole, $B_{12}N_{12,}$ and their complexes [35]. In order to find the most stable configuration, the adsorption process was evaluated at four different configurations. At first, all of the designed structures were optimized geometrically. Then, IR and frontier molecular orbital (FMO) and natural bond orbitals (NBO) computations were performed on them [3]. All of the computations were performed by Gaussian 16 software using the density functional theory method in the B3LYP/6-31G (d) level of theory [36]. This level of theory was chosen because in previous researches its results were inadmissible following the experimental findings. GuassSum software was employed for obtaining density of states (DOS) diagrams [37]. All of the calculations were done in the aqueous phase in the temperature range of 278.15-378.15 at 10˚ intervals.

The studied processes were as follows:

$$\text{Trinitroanisole}+B_{12}N_{12} \longrightarrow \text{Trinitroanisole-}B_{12}N_{12} \quad (1)$$

Equations 2-5 were employed for calculating adsorption energy values (E_{ad}) and thermodynamic parameters of the evaluated process including adsorption enthalpy changes (ΔH_{ad}), Gibbs free energy changes (ΔG_{ad}) and thermodynamic equilibrium constants (K_{th}) [3, 29, 30].

$$E_{ad} = \left(E_{(\text{Trinitroanisole}-B_{12}N_{12})} - \left(E_{(\text{Trinitroanisole})} + E_{(B_{12}N_{12})}\right)\right) \quad (2)$$

$$\Delta H_{ad} = \left(H_{(\text{Trinitroanisole}-B_{12}N_{12})} - \left(H_{(\text{Trinitroanisole})} + H_{(B_{12}N_{12})}\right)\right) \quad (3)$$

$$\Delta G_{ad} = \left(G_{(\text{Trinitroanisole}-B_{12}N_{12})} - \left(G_{(\text{Trinitroanisole})} + G_{(B_{12}N_{12})}\right)\right) \quad (4)$$

$$K_{th} = \exp\left(-\frac{\Delta G_{ad}}{RT}\right) \quad (5)$$

In the above-mentioned equations, E stands for the total electronic energy of each structure, H is the sum of the thermal enthalpy and total energy of the evaluated materials. The G also denotes the sum of the thermal Gibbs free energy and total energy for each of the studied structures. R is the ideal gas constants and T is the temperature [3, 33].

Frontier molecular orbital parameters such as bandgap (HLG), chemical hardness (η), chemical potential (μ), electrophilicity (ω) and the maximum transferred charge (ΔN_{max}) were calculated via equations 6-10 [28-31].

$$\text{HLG} = E_{LUMO} - E_{HOMO} \quad (6)$$

$$\eta = {}^{(E_{LUMO} - E_{HOMO})}/_{2} \quad (7)$$

$$\mu = {}^{(E_{LUMO} + E_{HOMO})}/_{2} \quad (8)$$

$$\omega = {}^{\mu^2}/_{2\eta} \quad (9)$$

$$\Delta N_{max} = -{}^{\mu}/_{\eta} \quad (10)$$

E_{LUMO} and E_{HOMO} in equations 6 to 8 denote the energy of the lowest unoccupied molecular orbital and the energy of the highest occupied molecular orbital respectively.

RESULTS AND DISCUSSION

Structural Properties

As can be seen from Fig. 1, trinitroanisole was inserted near the boron nitride cage at four different positions, for a more convenient understanding, each configuration was remarked by an abbreviated name. The naming method is explained in the following:

The A-Isomer abbreviation stands for the derivative in which the sixth carbon atom of trinitroanisole is inserted near the surface of the boron nitride cage. The B-Isomer symbol is considered for the derived product in which the explosive is placed near the adsorbent from its methyl group. C-Isomer also denotes the derivative in which the trinitroanisole was situated close to the $B_{12}N_{12}$ from its nitro group (the second nitrogen) and the D-Isomer abbreviation was selected for the complex in which the benzene ring of trinitroanisole is placed in parallel form near the surface of nanostructure.

The reported adsorption energy values in Table 1, were calculated via equation 2. As can be seen from the table, this parameter is considered

Table 1. The values of the total energy, adsorption energy, lowest frequency, bond lengths, weight, volume, and density for, trinitroanisole and its derived products with $B_{12}N_{12}$.

	Trinitroanisole	A-Isomer	B -Isomer	C-Isomer	D-Isomer	Bond order	Occupancy	Bond energy (a.u.)	Hybridization
Total energy (a.u)	-942.410	-1826.530	-1826.483	-1826.682	-1826.366	---	---	---	---
Adsorption energy (KJ/mol)	---	-540.740	-417.898	-941.149	-111.457	---	---	---	---
Lowest frequency (cm^{-1})	34.332	24.123	19.229	28.113	18.798	---	---	---	---
C_1-N_1 (Å)	1.511	1.524	1.563	1.542	1.537	---	---	---	---
C_5-N_2 (Å)	1.507	1.518	1.526	1.522	1.532	---	---	---	---
C_3-N_3 (Å)	1.511	1.532	1.541	1.548	1.536	---	---	---	---
N_1-O_1 (Å)	1.280	1.368	1.348	1.303	1.363	---	---	---	---
N_1-O_2 (Å)	1.276	1.318	1.339	1.293	1.334	---	---	---	---
N_2-O_1 (Å)	1.278	1.300	1.286	1.342	1.294	---	---	---	---
N_2-O_2 (Å)	1.278	1.297	1.293	1.282	1.293	---	---	---	---
N_3-O_1 (Å)	1.279	1.295	1.291	1.365	2.562	---	---	---	---
N_3-O_2 (Å)	1.276	1.291	1.286	1.332	1.334	---	---	---	---
C_6-B (Å)	---	1.589	---	---	---	1	1.99	-0.610	$Sp^{2.95}$
C_7-N (Å)	---	---	1.325	---	---	1	2.03	-0.595	$Sp^{2.99}$
N_2-B (Å)	---	---	---	1.608	---	1	1.94	-0.637	$Sp^{3.03}$
C_4-N (Å)	---	---	---	---	1.439	1	2.08	-0.489	$Sp^{2.946}$
Weight (amu)	243.131	525.932	525.932	525.932	525.932	---	---	---	---
Volume ($Å^3$)	193.590	417.211	416.490	414.324	411.340	---	---	---	---
Density=m/v (amu/$Å^3$)	1.256	1.261	1.263	1.269	1.279	---	---	---	---

negative for all of the configurations, therefore, it can be deduced that the adsorption process of trinitroanisole is experimentally feasible [26, 30]. Therefore, this nanostructure can be applied for the removal of trinitroanisole from the environmental specimens [3]. The highly negative adsorption energy values and the short bond lengths between the nanostructure and trinitroanisole indicate the interaction with the boron nitride cage and trinitroanisole is chemisorption and the results of NBO calculations also confirmed this finding. As it is obvious from the presented NBO results in Table 1. A covalent bond with SP^3 hybridization is formed between the adsorbate and BN nanocage in all of the evaluated conformers. Therefore, the interaction between trinitroanisole and $B_{12}N_{12}$ is not a Physisorption.

Because N-O, N-NO_2, and C-NO_2 bond lengths are appropriate standards for estimating the blasting power in the nitroaromatic explosives, after implementing geometrical optimization on the studied structures, the mentioned bond lengths were measured and tabulated in Table 1. As the provided data in Table 1 reveal, the N-O, N-NO_2, and C-NO_2 bond lengths have increased in trinitroanisole after the adsorbing on the surface of the boron nitride cage at all of the evaluated configurations. The incrementing of the referred bond lengths exhibits that the existed bonds between nitrogen and oxygen as well as nitrogen and carbon have become much weaker and they can be ruptured more easily by interacting with boron nitride cage. In other words, trinitroanisole complexes with $B_{12}N_{12}$ can take part in the combustion reaction more conveniently in comparison to the pure trinitroanisole and its blasting power have ameliorated substantially [30-33].

Density was the next investigated structural parameter which was obtained by dividing the weight of the structures to the calculated volumes after the optimization step. According to equations 11 and 12, density has a direct and obvious relationship with explosion velocity and detonation pressure [34].

$$D ¼ = 1.01(NM ½ Q ½)1/2(1 + 1.30\rho) \quad (11)$$

$$P ¼ = 1.558\, NM ½ Q ½ \rho 2 \quad (12)$$

In these formulas, D is the explosion velocity, P is the detonation pressure, M represents the average molecular weight of gaseous products, N stands for the number of moles of gaseous explosion products per gram of explosives, Q is the blasting Heat and ρ is the density of blasting material. As it can be seen from the table, the density of trinitroanisole has enhanced after adsorbing on the surface of $B_{12}N_{12}$. Among the studied derived products, D-isomer has the greatest one. Hence, coating trinitroanisole on the surface of the boron nitride cage leads to a significant rise in the explosion velocity and detonation pressure of the inspected blasting

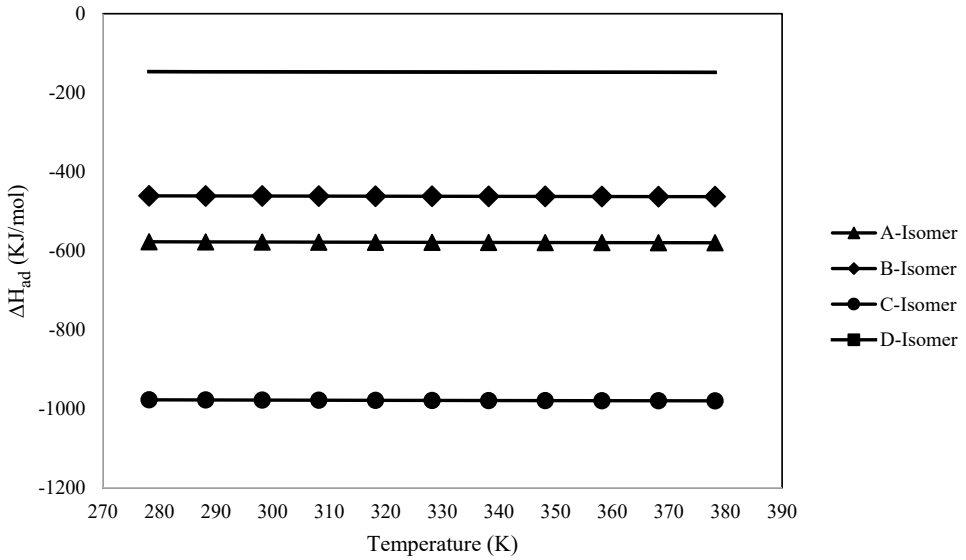

Fig. 2. The effect of temperature on the adsorption enthalpy changes (ΔH_{ad}) values in the temperature range of 278.15-378.15 at 10° intervals.

material in all of the configurations [3, 34, 30].

Thermodynamic Parameters of the Adsorption Process

The calculated ΔH_{ad} values and the effect of temperature on this parameter are depicted in Fig. 2. As can be seen, trinitroanisole adsorption on the surface of $B_{12}N_{12}$ is extremely exothermic at all of the conformers. In fact, the heat or energy is transferred from the system to the environment in the adsorption process. Therefore, this nanostructure can be used as a new sensing material for the construction of trinitroanisole thermal sensors. This type of sensors measures the amount of analyte by measuring the changes in the environmental temperature by a sensitive thermistor [31, 32]. Among the complexes, C-Isomer has the least enthalpy alterations values in comparison to other configurations. Hence, this derivative is more stable than others. The influence of temperature on this parameter was also investigated. As it is obvious from the table, by increasing temperature, ΔH_{ad} does not experience any tangible changes. Hence, based on this parameter, the optimum temperature for the adsorption process cannot be determined [3].

The presented ΔG_{ad} values in Fig. 3. shows that the trinitroanisole adsorption on the surface of $B_{12}N_{12}$ is spontaneously at all of the conformers due to the achieved negative Gibbs free energy changes. It seems the formation of C-Isomer is more spontaneous than other derived products because of its most negative ΔG_{ad} value. moreover, the highest Gibbs free energy is observed at D-Isomer. So, the interaction of trinitroanisole with adsorbent is weaker in this situation [24]. The influence of changing the temperature on this parameter was also evaluated and the results proved that by increasing temperature, ΔG_{ad} has incremented gradually. In other words, the adsorption process has become less spontaneous with temperature increasing. Hence, 278.15 K was selected as the optimum temperature for the adsorption of trinitroanisole on the surface of the adsorbent [25]. This phenomenon was expectable because trinitroanisole is more reactive at higher temperatures and it has more tendency to take part in combustion reactions. However, in lower temperatures, it is more stable and consequently can participate in other interactions more conveniently [26].

As can be observed from the presented thermodynamic equilibrium constants in Fig. 4, the trinitroanisole interaction with $B_{12}N_{12}$ is irreversible and non-equilibrium. The main advantage of K_{th} is that it shows the influence of temperature more sharply than other parameters. As it is obvious from Fig. 4, this parameter decreased remarkably by increasing temperature. Therefore, the adsorption process has become less irreversible and more equilibrium by increasing temperature. Hence, it can be concluded that 278.15 K is the best temperature for the adsorption of trinitroanisole on the surface of $B_{12}N_{12}$ [27, 28]. However, it should be noted that the adsorption process was evaluated only thermodynamically in this study and in order to obtain more definitive results, kinetic studies should also be carried out.

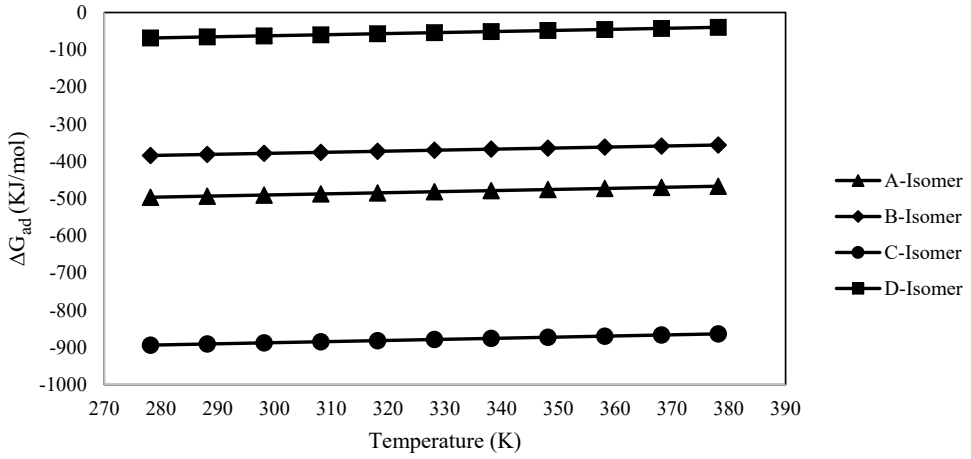

Fig. 3. The effect of temperature on the Gibbs free energy changes (ΔG_{ad}) values in the temperature range of 278.15-378.15 at 10° intervals.

Owing to the fact that the specific heat capacity has a clear relationship with heat sensitivity, this parameter was also calculated and the results presented in Fig. 5. Specific heat capacity is defined as the heat or energy that is needed for increasing the temperature of a certain amount of material to one Celsius degree. Hence, a compound with a higher C_V value will have a lower sensitivity to the heat because it requires higher energy to increase its temperature. On the other hand, a molecule with a low specific heat capacity value will be more sensitive to heat because its temperature can increase by a lower amount of heat. As can be seen from Fig. 5. the specific heat capacity has enhanced sharply after trinitroanisole interaction with boron nitride cage, in all of the conformers [20-25]. Hence, the heat sensitivity of trinitroanisole has declined substantially after adsorbing on the $B_{12}N_{12}$. The next point which can be perceived from Fig. 5, is that by growing temperature specific heat capacity values have also augmented linearly.

Frontier Molecular Orbital Analysis

As mentioned earlier, HOMO and LUMO are the highest occupied molecular orbital and the lowest unoccupied molecular orbital respectively. The energy discrepancy between these orbitals is known as an energy gap (HLG). HLG has an obvious relationship between conductivity and electrocatalytic activity. The molecules with low HLG values need lower energy for transferring their electrons from the ground state to the excited one in comparison to the compounds with higher HLG values. Therefore, a molecule with a little

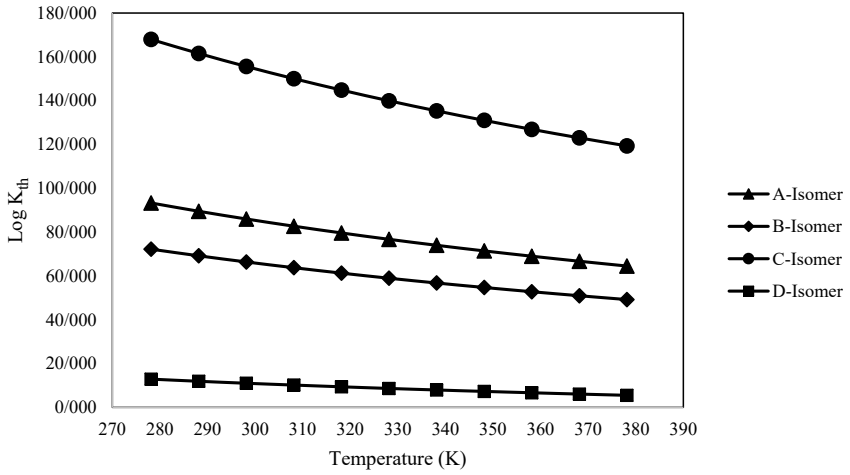

Fig. 4. The effect of temperature on the thermodynamic equilibrium constant (Log K_{th}) values in the temperature range of 278.15-378.15 at 10˚ intervals.

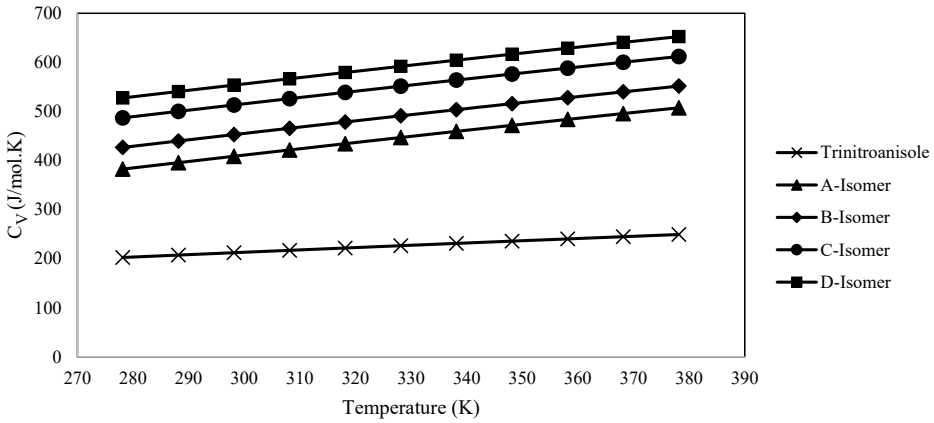

Fig. 5. The effect of temperature on the specific heat capacity (C_V) values in the temperature range of 278.15-378.15 at 10˚ intervals.

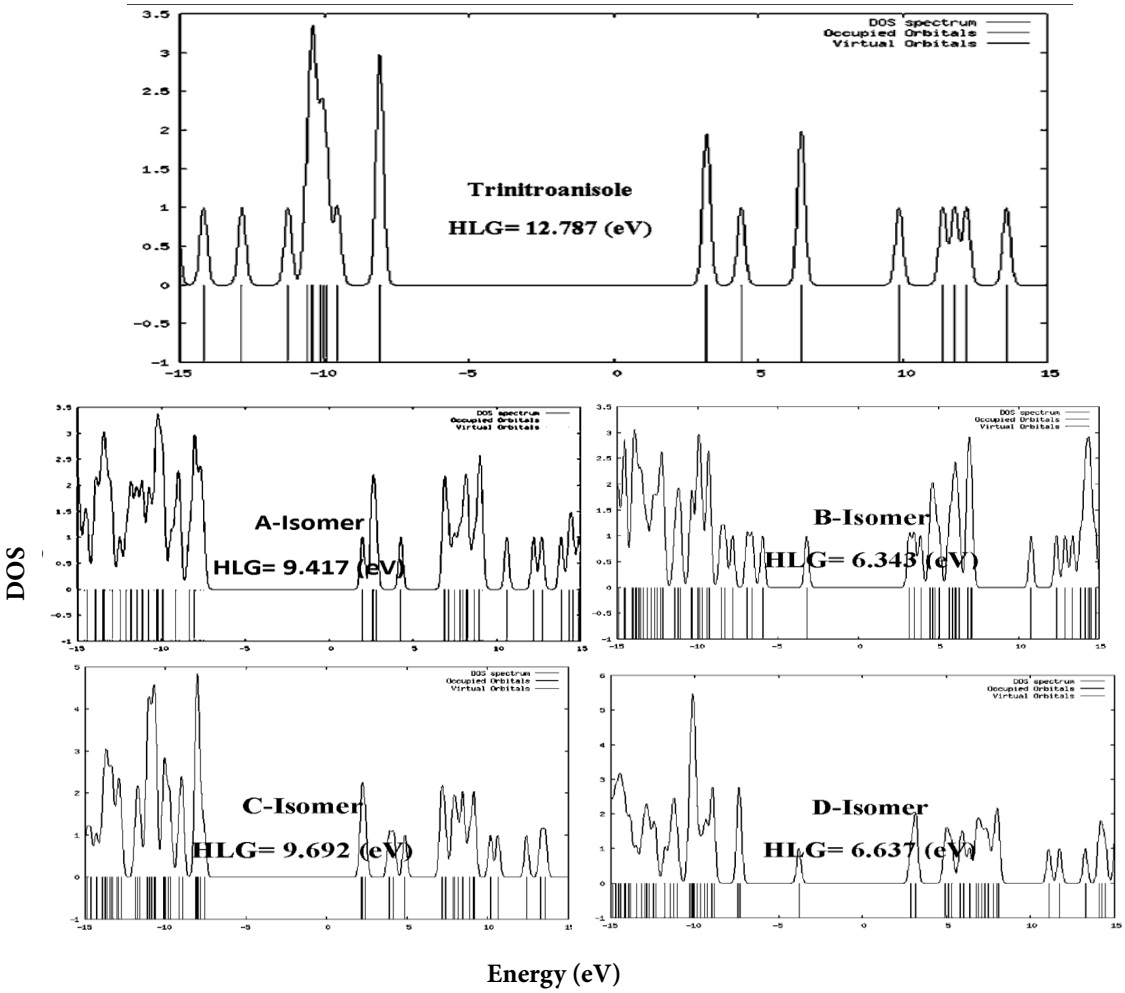

Fig. 6. The density of states (DOS) plots for trinitroanisole and its complexes with boron nitride cage

HLG value will have higher conductivity than a compound with a high amount of bandgap. As can be seen from the density of states (DOS) plots in Fig. 6. this parameter has experienced a sharp decrease after trinitroanisole adsorption on the $B_{12}N_{12}$ surface. In other words, the electrocatalytic performance has improved dramatically by the explosive interaction with $B_{12}N_{12}$. Therefore, it can be deduced that this nanocage can be employed for the detection of this energetic compound by electrochemical sensors [23-27].

Chemical hardness (η) was the next evaluated parameter which was calculated by equation 7. This variable has an obvious dependency on the reactivity. Soft molecules that have lower values of η will have more reactivity because they can change their electron density so conveniently. After all, electronic transmissions that are essential for the implementation of reaction can be done more easily in them. The presented results in Table 2, indicate that the reactivity of trinitroanisole has improved considerably after adsorbing on the surface of the boron nitride cage [35].

Electrophilicity (ω) and maximum transferred charge (ΔN_{max}) are good standards for estimating the tendency of a molecule towards electron. If a material has a great and positive value of ω and ΔN_{max} it will have more affinity for absorbing an electron. But, if a molecule has a low amount of these indices, it will act as an electron donor [27]. The obtained results in Table 2 exhibit that trinitroanisole can act as a Lewis acid or an electron acceptor because of its high electrophilicity and maximum transferred charge values. However, $B_{12}N_{12}$ can play the role of an electron donor because of its low electrophilicity. Therefore, it can be inferred that this nanocage and

Table 2. The calculatedE_H and EL, HLG, chemical hardness (η), electrophilicity index (ω), and the maximum amount of electronic charge index (ΔN_{max}) and dipole moment for trinitroanisole and its derivatives with boron nitride cage

	E_H (eV)	E_L (eV)	HLG (eV)	η (eV)	μ (eV)	ω (eV)	ΔN_{max} (eV)	Dipole moment (deby)	Zero point energy (KJ/mol)
Boron nitride cage	-8.290	6.690	14.980	7.490	-0.800	0.043	0.107	0.000	349.518
Trinitroanisole	-8.003	4.785	12.787	6.394	-1.609	0.202	0.252	1.840	405.780
A-Isomer	-7.428	1.989	9.417	4.708	-2.720	0.786	0.578	3.990	780.230
B-Isomer	-3.183	3.160	6.343	3.172	-0.012	0.000	0.004	13.393	738.412
C-Isomer	-7.551	2.141	9.692	4.846	-2.705	0.755	0.558	3.965	749.059
D-Isomer	-3.775	2.862	6.637	3.318	-0.456	0.031	0.138	6.448	739.750

the explosive can participate in electron transfer reactions. Hence, the boron nitride cage is an excellent sensing material for the construction of new trinitroanisole electrochemical sensors [30, 33]. The next matter that can be understood from the provided data in Table 2, is that the electrophilicity and also maximum transmitted charge enjoy a substantial increase in the boron nitride cage complexes with trinitroanisole. Therefore, the pure explosive is less electrophile than its derived products with $B_{12}N_{12}$ [3].

The dipole moment is a key clue that shows the solubility of the studied structures. A molecule with a high dipole moment will be more soluble in the polar solvents like water. On the other hand, a low amount of dipole moment indicates the poor solubility in polar solvents. As it is obvious, the dipole moment of $B_{12}N_{12}$ is zero. Hence, this nanostructure is insoluble in water. This result is too interesting because most of the electrochemical sensors lose their sensitivity and reproducibility after a short time due to the leakage of the recognition element from the membrane to the sample solution. Therefore, sensing materials with a lower solubility in polar solvents are more suitable for the construction of new sensors. Fortunately, the boron nitride cage meets this requirement. In addition, the dipole moment of trinitroanisole has improved dramatically after its interaction with $B_{12}N_{12}$. Hence, the explosive has become more soluble in water after adsorbing on the boron nitride cage surface [33].

CONCLUSION

Trinitroanisole is a hazardous environmental contaminant that has adverse effects on the health of human beings. Therefore, its removal and determination are of vital importance. In this regard, the applicability of boron nitride nanocage as an adsorbent and sensing material for trinitroanisole was studied by the DFT method in the B3LYP/6-31G (d) level of theory. The results indicated trinitroanisole interaction with $B_{12}N_{12}$ is experimentally possible, spontaneously, irreversible, and non-equilibrium. Besides, the interaction of trinitroanisole with boron nitride cage is exothermic and this nanostructure can be used for the thermal detection of trinitroanisole. The temperature influence on the studied process was also checked out and it was found out 278.15 K is the optimum temperature. The specific heat capacity values demonstrated that coating trinitroanisole on the $B_{12}N_{12}$ surface leads to a significant decrease in the heat sensitivity of the evaluated explosive. The structural features such as bond lengths and density values substantiated that the $B_{12}N_{12}$ complexes with trinitroanisole have higher detonation velocity, blasting pressure, and explosive power in comparison to pure trinitroanisole. The frontier molecular orbital parameters also exhibited that boron nitride cage can be utilized as a sensing material for trinitroanisole detection.

CONFLICT OF INTEREST

The authors declare no conflict of interest in this study.

REFERENCES

1. Cady HH. The crystal structure of N-methyl-N-2,4,6-tetranitroaniline (tetryl). Acta Crystallographica. 1967;23(4):601-9.
2. Hariharan PC, Koski WS, Kaufman JJ, Miller RS. Ab initioMODPOT/VRDDO/MERGE calculations on energetic compounds. III. Nitroexplosives: Polyaminopolynitrobenzenes (including DATB, TATB, and tetryl). International Journal of Quantum Chemistry. 1983; 23(4) :1493-504.
3. Jalali Sarvestani, M. R., R. Ahmadi, 2020. Adsorption of Tetryl on the Surface of $B_{12}N_{12}$: A Comprehensive DFT Study. Chemical Methodologies, 4 (1): 40-54.
4. Enlow MA. Binding of TNT to amplifying fluorescent polymers: An ab initio and molecular dynamics study. Journal of Molecular Graphics and Modelling. 2012;33:12-8.
5. Ahmadi, R., 2017. Study of thermodynamic parameters of (TATB) and its fullerene derivatives with different number of Carbon (C20, C24, C60), in different conditions of temperature, using density functional theory. International Journal of Nano Dimension, 8 (3): 250-256.
6. Myers SR, Spinnato JA. Metabolism, tissue distribution, and pharmacokinetics of N-methyl-N-2,4,6-tetranitroaniline (tetryl). Environmental Toxicology and Pharmacology. 2007;24(3):206-11.
7. Khue DN, Lam TD, Van Chat N, Bach VQ, Minh DB, Loi VD, et al. Simultaneous degradation of 2,4,6-trinitrophenyl-N-methylnitramine (Tetryl) and hexahydro-1,3,5-trinitro-1,3,5 triazine (RDX) in polluted wastewater using some advanced oxidation processes. Journal of Industrial and Engineering Chemistry. 2014;20(4):1468-75.
8. Todde G, Jha SK, Subramanian G, Shukla MK. Adsorption of TNT, DNAN, NTO, FOX7, and NQ onto cellulose, chitin, and cellulose triacetate. Insights from Density Functional Theory calculations. Surface Science. 2018;668:54-60.
9. Reddy TV, Olson GR, Wiechman B, Reddy G, Torsella J, Daniel FB, et al. Toxicity of Tetryl (N-Methyl-N,2,4,6–Tetranitroaniline) in F344 Rats. International Journal of Toxicology. 1999;18(2):97-107.
10. Alizadeh T, Zare M, Ganjali MR, Norouzi P, Tavana B. A new molecularly imprinted polymer (MIP)-based electrochemical sensor for monitoring 2,4,6-trinitrotoluene (TNT) in natural waters and soil samples. Biosensors and Bioelectronics. 2010;25(5):1166-72.
11. Hilton J, Swanston CN. Clinical Manifestations of Tetryl and Trinitrotoluene. BMJ. 1941;2(4214):509-10.
12. Tredici I, Merli D, Zavarise F, Profumo A. α-Cyclodextrins chemically modified gold electrode for the determination of nitroaromatic compounds. Journal of Electroanalytical Chemistry. 2010;645(1):22-7.
13. Stringer RC, Gangopadhyay S, Grant SA. Detection of Nitroaromatic Explosives Using a Fluorescent-Labeled Imprinted Polymer. Analytical Chemistry. 2010;82 (10):4015-9.
14. Rodgers JD, Bunce NJ. Treatment methods for the remediation of nitroaromatic explosives. Water Research. 2001;35(9):2101-11.
15. Heidary, R., 2013. Simultaneous Determination of Carbazoles in Water Samples by Cloud Point Extraction Coupled to HPLC. Journal of Applied Chemical Research, 7 (2): 21-31.
16. Pan Y, Zhu W, Xiao H. Theoretical studies of a series of azaoxaisowurtzitane cage compounds with high explosive performance and low sensitivity. Computational and Theoretical Chemistry. 2017;1114:77-86.
17. Han G, Gou R-j, Ren F-d, Zhang S-h, Wu C-l, Zhu S-f. Theoretical investigation into the influence of molar ratio on binding energy, mechanical property and detonation performance of 1,3,5,7-tetranitro-1,3,5,7-tetrazacyclo octane (HMX)/1-methyl-4,5-dinitroimidazole (MDNI) cocrystal explosive. Computational and Theoretical Chemistry. 2017;1109:27-35.
18. Ma P, Pan Y, Jiang J-c, Zhu S-g. Molecular Dynamic Simulation and Density Functional Theory Insight into the Nitrogen Rich explosive 1,5-diaminotetrazole(DAT). Procedia Engineering. 2018;211:546-54.
19. Wang K, Fu X-l, Tang Q-f, Li H, Shu Y-j, Li J-q, et al. Theoretical investigations on novel energetic salts composed of 4-nitro-7-(4-nitro-1,2,3-triazol-1-olate)-furazano[3,4-d] pyridazine-based anions and ammonium-based cations. Computational Materials Science. 2018;146:230-9.
20. Sviatenko LK, Gorb L, Shukla MK, Seiter JM, Leszczynska D, Leszczynski J. Adsorption of 2,4,6,8,10,12-hexanitro-2,4,6,8,10,12-hexaazaisowurtzitane (CL-20) on a soil organic matter. A DFT M05 computational study. Chemosphere. 2016;148:294-9.
21. Allis DG, Zeitler JA, Taday PF, Korter TM. Theoretical analysis of the solid-state terahertz spectrum of the high explosive RDX. Chemical Physics Letters. 2008;463(1-3):84-9.
22. Jain P, Sahariya J, Mund HS, Sharma M, Ahuja BL. Ab initio calculations for electronic and optical properties of explosive silver azide. Computational Materials Science. 2013; 72:101-6.
23. Fayet G, Joubert L, Rotureau P, Adamo C. On the use of descriptors arising from the conceptual density functional theory for the prediction of chemicals explosibility. Chemical Physics Letters. 2009;467(4-6):407-11.
24. Konek CT, Mason BP, Hooper JP, Stoltz CA, Wilkinson J. Terahertz absorption spectra of 1,3,5,7-tetranitro-1,3,5,7-tetrazocane (HMX) polymorphs. Chemical Physics Letters. 2010;489(1-3):48-53.
25. Bahrami A, Seidi S, Baheri T, Aghamohammadi M. A first-principles study on the adsorption behavior of amphetamine on pristine, P- and Al-doped B12N12 nano-cages. Superlattices and Microstructures. 2013;64:265-73.
26. Baei MT. B12N12 sodalite like cage as potential sensor for hydrogen cyanide. Computational and Theoretical Chemistry. 2013;1024:28-33.
27. Esrafili MD. N 2 O reduction over a fullerene-like boron nitride nanocage: A DFT study. Physics Letters A. 2017;381(25-26):2085-91.
28. Soltani A, Baei MT, Mirarab M, Sheikhi M, Tazikeh Lemeski E. The electronic and structural properties of BN and BP nano-cages interacting with OCN−: A DFT study. Journal of Physics and Chemistry of Solids. 2014;75(10):1099-105.
29. Jalali Sarvestani, M. R., R. Ahmadi, 2019. Investigating the influence of doping graphene with silicon and germanium on the adsorption of silver (I). Journal of Water and Environmental Nanotechnology, 4 (1): 48-59.
30. Jalali Sarvestani, M. R., M. Gholizadeh Arashti and Mohasseb,

B., 2020. Quetiapine Adsorption on the Surface of Boron Nitride Nanocage ($B_{12}N_{12}$): A Computational Study. International Journal of New Chemistry, 7 (2): 87-100.

31. Culebras M, López AM, Gómez CM, Cantarero A. Thermal sensor based on a polymer nanofilm. Sensors and Actuators A: Physical. 2016;239:161-5.
32. Mohasseb, A., 2019. Adsorption of Tetryl on the Surface of Carbon Nanocone: A Theoretical Investigation. International Journal of New Chemistry, 6(4): 215-223.
33. Jalali Sarvestani, M. R., L. Hajiaghbabaei, J. Najafpour and S. Suzangarzadeh, 2018. 1-(6-choloroquinoxaline-2-yl) Hydrazine as an Excellent Ionophore for Ppreparation of a Cobalt Selective Electrode and Potentiometric Measuring of Vitamin B12 in Pharmaceutical Samples. Analytical and Bioanalytical Electrochemistry, 10 (6): 658-674.
34. Ravi P, Gore GM, Tewari SP, Sikder AK. DFT study on the structure and explosive properties of nitropyrazoles. Molecular Simulation. 2012;38(3):218-26.
35. GaussView, Version 6.1, Roy Dennington, Todd A. Keith, John M. Millam, Semichem Inc., Shawnee Mission, KS, 2016.
36. Gaussian 16, Revision C.01, M. J. Frisch, G. W. Trucks, H. B. Schlegel, G. E. Scuseria, M. A. Robb, J. R. Cheeseman, G. Scalmani, V. Barone, G. A. Petersson, H. Nakatsuji, X. Li, M. Caricato, A. V. Marenich, J. Bloino, B. G. Janesko, R. Gomperts, B. Mennucci, H. P. Hratchian, J. V. Ortiz, A. F. Izmaylov, J. L. Sonnenberg, D. Williams-Young, F. Ding, F. Lipparini, F. Egidi, J. Goings, B. Peng, A. Petrone, T. Henderson, D. Ranasinghe, V. G. Zakrzewski, J. Gao, N. Rega, G. Zheng, W. Liang, M. Hada, M. Ehara, K. Toyota, R. Fukuda, J. Hasegawa, M. Ishida, T. Nakajima, Y. Honda, O. Kitao, H. Nakai, T. Vreven, K. Throssell, J. A. Montgomery, Jr., J. E. Peralta, F. Ogliaro, M. J. Bearpark, J. J. Heyd, E. N. Brothers, K. N. Kudin, V. N. Staroverov, T. A. Keith, R. Kobayashi, J. Normand, K. Raghavachari, A. P. Rendell, J. C. Burant, S. S. Iyengar, J. Tomasi, M. Cossi, J. M. Millam, M. Klene, C. Adamo, R. Cammi, J. W. Ochterski, R. L. Martin, K. Morokuma, O. Farkas, J. B. Foresman, and D. J. Fox, Gaussian, Inc., Wallingford CT, 2016.
37. O'Boyle NM, Tenderholt AL, Langner KM. cclib: A library for package-independent computational chemistry algorithms. Journal of Computational Chemistry. 2008;29(5):839-45.